High-precision U-Pb zircon ages and geochemical data from igneous rocks spatially associated with the Llewellyn-Tally Ho deformation corridor, northwestern British Columbia and southern Yukon

L. Ootes, S. Castonguay, F. Devine, C. Wall, S. Zhang

British Columbia Geological Survey est. 1895

BRITISH COLUMBIA
Ministry of Mining and Critical Minerals

GeoFile 2026-12

Ministry of Mining and Critical Minerals
Mines Competitiveness and Authorizations Division
British Columbia Geological Survey

Ootes, L., Castonguay, S., Devine, F. Wall, C., and Zhang, S. 2026. High-precision U-Pb zircon ages and geochemical data from igneous rocks spatially associated with the Llewellyn-Tally Ho deformation corridor, northwestern British Columbia and southern Yukon. British Columbia Ministry of Mining and Critical Minerals, British Columbia Geological Survey GeoFile 2026-12,7p.

Front cover:
Northwest striking, steeply dipping brittle fabric of the Llewellyn fault crosscutting Lewes River Group volcanic rocks on Mount Hodnett, southern Yukon. View is to the south.

Back cover
Gabbroic White Pass dike (Eocene) east of Highway 2 and southern Tutshi Lake.

BRITISH COLUMBIA

Ministry of Mining and Critical Minerals

High-precision U-Pb zircon ages and geochemical data from igneous rocks spatially associated with the Llewellyn-Tally Ho deformation corridor, northwestern British Columbia and southern Yukon

L. Ootes
S. Castonguay
F. Devine
C. Wall
S. Zhang

Ministry of Mining and Critical Minerals
British Columbia Geological Survey
GeoFile 2026-12

High-precision U-Pb zircon ages and geochemical data from igneous rocks spatially associated with the Llewellyn-Tally Ho deformation corridor, northwestern British Columbia and southern Yukon

L. Ootes[1a], S. Castonguay[2], F. Devine[3], C. Wall[4], and S. Zhang[5]

[1] British Columbia Geological Survey, Ministry of Mining and Critical Minerals, Victoria, BC, V8W 9N3
[2] Geological Survey of Canada, Natural Resources Canada, Québec, QC, G1K9A9
[3] Merlin Geoscience, 2946 Enderby Mabel Lake Road, Enderby, BC, V4Y 4L3
[4] Pacific Centre for Isotopic and Geochemical Research, Department of Earth, Ocean and Atmospheric Sciences, Vancouver, BC, V6T 1Z4
[5] Isotope Geochronology and Geochemistry Research Centre, Department of Earth Sciences, Carleton University, Ottawa, ON, K1S 5B6
[a] corresponding author: Luke.Ootes@gov.bc.ca

Recommended citation: Ootes, L., Castonguay, S., Devine, F. Wall, C., and Zhang, S. 2026. High-precision U-Pb zircon ages and geochemical data from igneous rocks spatially associated with the Llewellyn-Tally Ho deformation corridor, northwestern British Columbia and southern Yukon. British Columbia Ministry of Mining and Critical Minerals, British Columbia Geological Survey GeoFile 2026-12,7p.

Abstract
High-precision U-Pb zircon geochronologic data and whole-rock major, trace, rare-earth element, and radiogenic isotope (Sr, Nd, Pb) geochemical data support ongoing studies along the Llewellyn-Tally Ho deformation corridor, northwestern British Columbia and southern Yukon. This corridor is spatially associated with a variety of gold prospects and minor past producers. Eleven new U-Pb zircon results, obtained by the CA-ID-TIMS method, provide crystallization ages for rocks along the corridor. We also present geochemical data from the Sloko Group volcanic rocks and White Pass dikes (Eocene), which are locally spatially related to mineralization.

Keywords: Llewellyn, Tally-Ho, geochronology, geochemistry, CA-ID-TIMS, Eocene

1. Introduction

In 2016, the British Columbia Geological Survey and Geological Survey of Canada initiated a three-year project in northwest British Columbia and southern Yukon (Fig. 1) to better understand the geology and mineralization along the Llewellyn-Tally Ho deformation corridor (Fig. 2; Ootes et al., 2017, 2018; Castonguay et al., 2020). Herein (BCGS_GF2026.zip) we present high-precision U-Pb zircon analyses from ten samples collected during mapping that help constrain the timing of deformation along the corridor. Four of the sample results were previously published (Ootes et al., 2018). In addition, we report geochemical data from volcanic rocks of the Sloko Group volcanic rocks and White Pass dikes (Eocene), which locally are spatially associated with mineralization in the study area.

2. Geology

The Llewellyn fault extends along strike northwest from British Columbia to the Tally-Ho shear zone in Yukon. In general, this deformation zone marks the boundary between the Nisling terrane to the west and Stikine terrane to the east (Fig. 2; Hart and Radloff, 1990; Mihalynuk et al., 1999; Tizzard et al., 2009) and is spatially associated with a variety of gold prospects and minor past producers. A complete overview of the geology can be found in Ootes et al. (2018) and Castonguay et al. (2020).

3. Geochronology

3.1. U-Pb zircon analytical methods: chemical abrasion isotope dilution thermal ionization mass spectrometry (CA-ID-TIMS)

Alteration and lichen-free samples were prepared in the field as chips then bagged and sealed. At The University of British Columbia, samples underwent standard mineral separation procedures, and zircon crystals were handpicked in alcohol. The procedures described here are modified from Mundil et al. (2004), Mattinson, (2005), and Scoates and Friedman (2008). The clearest, crack- and inclusion-free grains were selected, photographed, and then annealed in quartz glass crucibles at 900˚C for 60 hours. Annealed grains were transferred into 3.5 mL PFA screwtop beakers; ultrapure HF (up to 50% strength, 500 mL) and HNO_3 (up to 14 N, 50 mL) were added and caps closed finger tight. The beakers were placed in 125 mL PTFE liners (up to four per liner) and about 2 mL HF and 0.2 mL HNO_3 (of the same strength as the acid in the beakers) were added to the liners. The liners were slid into stainless steel

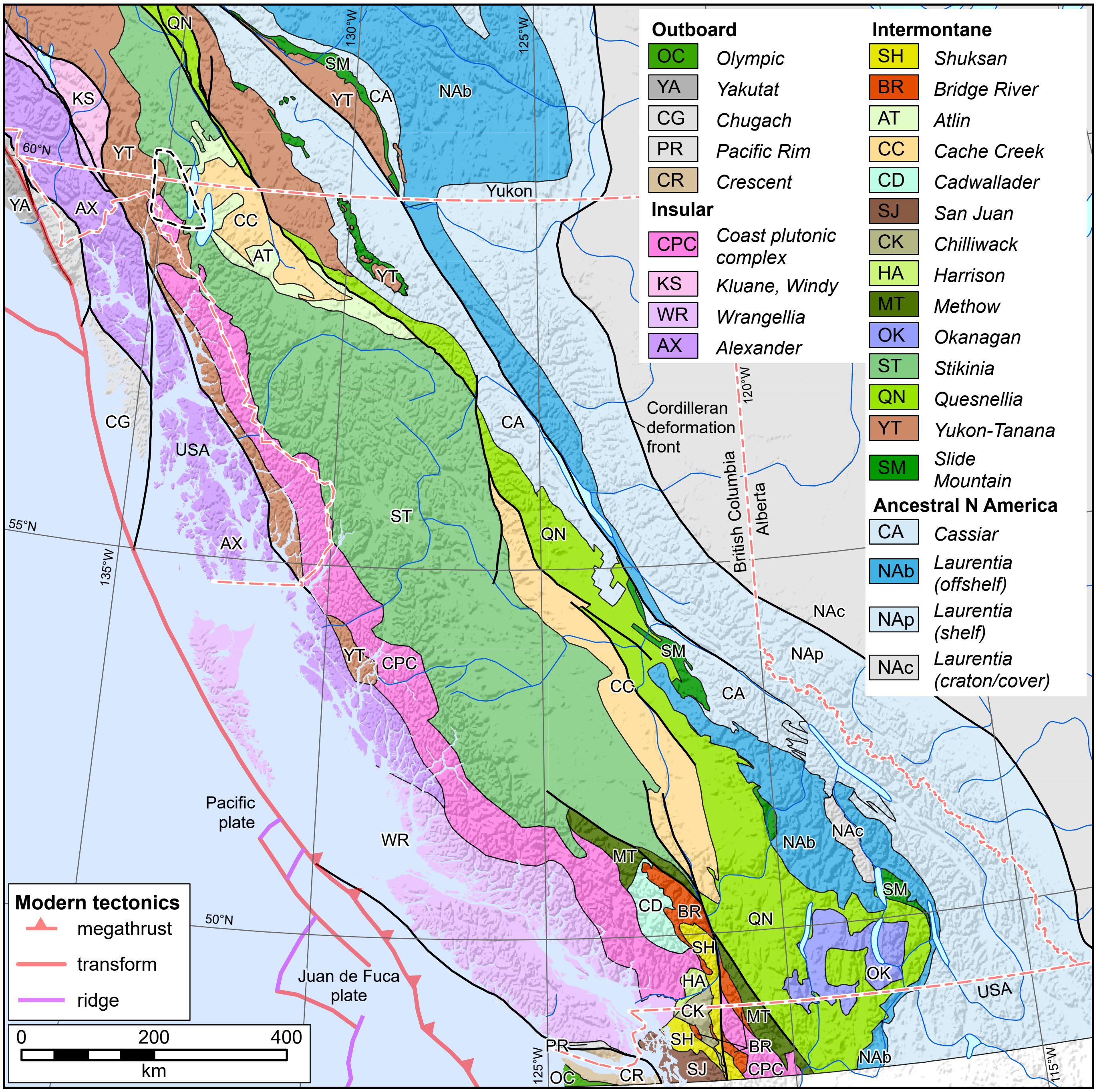

Fig. 1. Location of this study in northwest British Columbia and southern Yukon (coarse dashed line). Terrane boundaries after Colpron (2020).

Parr™ high-pressure dissolution devices, which were sealed and brought to a maximum of 200˚C for 8-16 hours (typically 190˚C for 12 hours). Beakers were removed from liners and zircon separated from leachate. Zircon grains were rinsed with >18 MΩ.cm water and subboiled acetone. Then 2 mL of subboiled 6N HCl was added and the beakers were set on a hotplate at 80˚-130˚C for 30 minutes and again rinsed with water and acetone. Masses were estimated from the dimensions (volumes) of grains. Single grains were transferred into clean 300 mL PFA microcapsules (crucibles), and 50 mL 50% HF and 5 mL 14 N HNO_3 were added. Each was spiked with a $^{233-235}U$-^{205}Pb tracer solution (EARTHTIME ET535), capped and again placed in a Parr liner (8-15 microcapsules per liner). HF and nitric acids in a 10:1 ratio, respectively, were added to the liner, which was then placed in a Parr high-pressure device, and dissolution was achieved at 220˚C for 40 hours. The resulting solutions were dried on a hotplate at 130˚C, 50 mL 6N HCl was added to microcapsules and fluorides were dissolved in high-pressure Parr devices for 12 hours at 180˚C. HCl solutions were transferred into clean 7 mL PFA beakers and dried with 2 mL of 0.5 N H_3PO_4. Samples were loaded onto degassed, zone-refined Re filaments in 2 mL of silicic acid emitter (Gerstenberger and Haase, 1997).

Isotopic ratios were measured with a single collector VG 54R thermal ionization mass spectrometer equipped with analogue Daly photomultiplier. Analytical blanks were 0.1 pg

Fig. 2. U-Pb zircon sample locations (red triangles) along the Llewellyn-Tally Ho deformation corridor (strands in blue; after Hart and Radloff, 1990 and Mihalynuk et al., 1999).

for U and up to 1.1 pg for Pb. U fractionation was determined directly on individual runs using the EARTHTIME ET535 mixed $^{233\text{-}235}$U-^{205}Pb isotopic tracer, and Pb isotopic ratios were corrected for fractionation of 0.25 ± 0.04%/amu, based on replicate analyses of NBS-982 reference material and the values recommended by Thirlwall (2000). Data reduction employed the Excel-based program of Schmitz and Schoene (2007). Unless otherwise noted all errors are quoted at the 2 sigma or 95% level of confidence. Isotopic dates were calculated with the decay constants l_{238}=1.55125E-10 and l_{235}=9.8485E-10 (Jaffe et al, 1971) and a ^{238}U/^{235}U ratio of 137.88. EARTHTIME U-Pb synthetic solutions were analyzed on an on-going basis to monitor the accuracy of results.

4. U-Pb zircon results

U-Pb zircon data, concordia and weighted mean plots, and outcrop photographs are in Appendix 1. The calculated ^{206}Pb/^{238}U weighted mean ages in the data tables are the best estimates of crystallization age of the rocks. All sample coordinates are in UTM Zone 8, NAD83.

4.1. Sample 17lo27, south end of Tagish Lake (542061mE, 6590433mN)

A composite gneiss assigned to the Boundary Ranges metamorphic suite outcrops immediately west of the Llewellyn fault near the Wann River at the south end of Tagish Lake. The gneiss consists of an amphibolite phase with local garnet that is strongly deformed together with a younger granodiorite. The gneissic fabric is 115°/57°SW and is crosscut by quartz veins. Sample 17lo27 is from the granodiorite.

Six zircon crystals were analyzed and yield consistent overlapping U-Pb dates and a weighted mean age of 184.74 ± 0.10 Ma (MSWD=1.27; n=5/5), which is interpreted to represent the crystallization age of the granodiorite phase.

4.2. 16lo18b and 18lo5, 2km south of Racine Lake

4.2.1. 16lo18b (526115mE 6617834mN); previously reported in Ootes et al. (2018)

Southwest of Racine Lake and directly east of Teepee Peak is a zone of imbricated Stuhini Group and minor Laberge Group rocks (Mihalynuk et al., 1999). The best exposures are on a hummock-like ridge that is transected by the brittle Llewellyn fault and related splays. The western-most splay separates Stuhini and Laberge group rocks from Boundary Ranges metamorphic suite rocks (Mihalynuk et al., 1999). Outcrops along the ridge contain a ridge-parallel foliation (~135°/90°) that is locally affected by steeply plunging minor folds. The rock types in the west are predominantly argillite and in the east black shale (slate) and marble. An intermediary unit of 'rhyolite' and associated rocks was identified by Mihalynuk et al. (1999) and during this study. The rhyolite unit weathers chalky white, contains plagioclase and quartz phenocrysts, and is commonly moderately to strongly foliated. The rhyolite is also carbonate altered, potentially related to brittle faulting along this zone. A sample of massive rhyolite with carbonate alteration was selected for geochronology.

Only two of six zircons survived the journey from separation to mass spectrometry but yield overlapping and concordant U-Pb ages. A ^{206}Pb/^{238}U weighted mean (n=2) of the analyses indicate a crystallization age of 120.53 ± 0.19 Ma (MSW=0.86; Ootes et al., 2018). Given the result in section 4.2.2., we interpret these as inherited zircons (Castonguay et al., 2020).

4.2.2. 18lo5 (526082mE, 6617767mN)

In 2018, we resampled the carbonate-altered rhyolite from site 75m to the southwest of sample 16lo18b(section 4.2.1). This sample yielded zircon and four were analyzed with near overlapping results. A weighted mean of these yields an age of 110.18 ± 0.20 Ma (MSWD=1.56; n=2/4). The combination of the high MSWD of this result, and the misfit of the result of this sample (ca. 111 Ma) versus the 16lo18b result (ca. 121 Ma), is best interpreted to indicate these rocks are younger than 110 Ma.

4.3. 17lo10 and 17lo16, Mount Hodnett, Yukon

4.3.1. 17lo10 (488346mE, 6686946NmN)

On the southwestern ridgeline of Mount Hodnett (Yukon), strongly deformed sedimentary and volcanic rocks of the Lewes River Group (Triassic) are cut by medium to coarse-grained quartz monzonite of the Whitehorse intrusive suite. The deformed supracrustal rocks comprise the Tally-Ho shear zone. At the margin of the sheared intrusive contact, the quartz monzonite contains a moderate foliation (~165°/75°SE), defined by biotite, that parallels the fabric in the supracrustal rocks. Farther to the west, in the body of the intrusive rocks, the foliation progressively decreases in intensity and disappears. As the quartz monzonite and Lewes River Group supracrustal rocks apparently share the same ductile fabric, the crystallization age of the quartz monzonite represents a maximum age for the preserved deformation.

A sample of the quartz monzonite was collected from this location and five zircons were analyzed. Four concordant overlapping results yield a weighted mean age of 98.62 ± 0.06 Ma (MSWD=0.64; n=4/5), which is interpreted as the crystallization age of the quartz monzonite. One single zircon is slightly older and is interpreted as an antecryst.

4.3.2. 17lo16 (488484mE, 6687088mN)

On Mount Hodnett, 200m northeast of sample 17lo10 (section 4.3.1.), an 8m wide, a fine to medium-grained feldspar porphyritic monzonite dike cuts deformed Lewes River Group supracrustal rocks. The core of the dike is mostly massive to weakly foliated (defined by aligned amphibole and biotite grains) and the dike is locally folded.

A sample of the dike was collected and five zircons were analyzed. An older grouping of three zircons yield overlapping results at ca. 98.75 Ma and two younger separate zircons yield overlapping results with a weighted mean age of 98.34 ± 0.1 Ma (MSWD=1.32; n=2/5). This is interpreted to represent the crystallization age of the dike.

4.4. 16lo11b (507977mE, 6642004mN); previously reported in Ootes et al. (2018)

At Bennett plateau, strongly deformed metasedimentary rocks of the Stuhini Group are crosscut by 2 m-wide quartz-feldspar- biotite-phyric intrusion with a fine-grained siliceous groundmass (granodiorite porphyry). The metasedimentary rocks contain quartz-actinolite veins that were folded and boudinaged. The area that contains these veins has been termed the 'Skarn zone'. The unfoliated granodiorite intrusion parallels the host rock fabrics but post-dates the ductile deformation (see Figure 5 in Ootes et al., 2018).

A sample of the granodiorite porphyry yielded good-quality igneous zircons. Four zircons were selected for analysis and yield overlapping, concordant results. A weighted mean age of 76.30 ± 0.05 Ma (MSWD=1.27; n=4) is interpreted as the crystallization of the intrusion (Ootes et al., 2018). This intrusion provides a minimum age of ca. 76 Ma for ductile deformation.

4.5. 16lo5b (515870mE, 6630703mN); previously reported in Ootes et al. (2018)

West of Moon Lake, along the trace of the Llewellyn fault, a fine- to medium-grained, weakly porphyritic (~0.5 cm-wide feldspar) granodiorite (unit Mgd in Mihalynuk et al., 1999), with moderate carbonate alteration and partially chloritized biotite and hornblende, cuts across the contact between the Stuhini Group and the Boundary Ranges metamorphic suite. The eastern contact of the granodiorite is parallel to bedding and foliation in Stuhini Group argillite; the granodiorite lacks a foliation and post-dates the ductile deformation preserved in the host argillite. The granodiorite is crosscut by a southeast-striking brittle fault, identifiable in the outcrop as a 2 m-wide zone of fault gouge with intense fracturing and carbonate alteration (see Figure 4a in Ootes et al., 2017).

A sample of least-altered granodiorite from near the contact with the host argillite yielded good-quality igneous zircon, and five single grains were selected for analysis. The results are concordant to slightly discordant and have a range of ages, from ca. 92 Ma to 74 Ma. The youngest zircon, at 73.94 ± 0.28 Ma, gives the maximum time of crystallization of the granodiorite sample. Older zircons with marginally concordant to slightly discordant results of ca. 76 Ma (n=3) and ca. 90 Ma are interpreted as xenocrysts, or as composite grains with older inherited cores and younger rims (Ootes et al., 2018).

4.6. 16lo20a, 16lo22, and 17lo26

4.6.1. 16lo20a (507640mE, 6647500mN); previously reported in Ootes et al. (2018)

East of Bennet Lake and south of the BC-Yukon border, intrusive rocks of the Sloko-Hyder intrusive suite (Paleogene) and Late Cretaceous intrusive rocks cut foliated Laberge Group metasedimentary rocks. At location 16lo20a, the unit was mapped as Late Cretaceous to Tertiary (unit LKqm in Mihalynuk et al., 1999). The granite does not contain a foliation or display evidence of brittle faulting.

A sample of a medium-grained granite with K-feldspar phenocrysts was collected for dating and five prismatic grains were analyzed. Three zircon grains overlap on concordia and yield a weighted mean of 56.58 ± 0.07 Ma (MSWD=0.36; n=3/5), interpreted as the crystallization age of the granite. Two marginally slightly older results are interpreted as antecrysts (Ootes et al., 2018).

4.6.2. 16lo22 (507264mE, 6649186mN); previously reported in Ootes et al. (2018)

East of Bennett Lake and 2 km south of the British Columbia-Yukon border an equigranular biotite-hornblende granite was collected from the Sloko-Hyder intrusive suite. The granite lacks a ductile fabric but contains closely spaced (<30 cm) brittle fractures at 360°/65°E, which align along the trend of and are probably related to the Llewellyn fault.

The sample yielded prismatic igneous zircons, and five single grains were selected for analysis. The results overlap on concordia and a weighted mean of the youngest four zircons yields a crystallization age of 56.46 ± 0.06 Ma (MSWD=0.95; n=4/5). One result is slightly older (56.76 Ma) and interpreted as an antecryst.

4.6.3. 17lo26 (511111mE, 6641345mN)

Near the west side of Tutshi Lake, ~350m west of Highway 2, granitic rocks cut Laberge Group sedimentary rocks. The Llewellyn fault truncates the western margin of the granite pluton and occurs within a deeply incised linear valley. Triassic-Jurassic supracrustal rocks occur on the west side of the fault. Because this granitic unit is cut by the fault, its crystallization age provides a maximum time of brittle deformation along the Llewellyn fault.

A sample of medium-grained K-feldspar and plagioclase porphyritic biotite granite was collected. Five zircons were analyzed, and single concordant results range from ca. 57.25 to 56.15 Ma. The best interpretation for the crystallization age of this rock is from the youngest single zircon, with a $^{206}Pb/^{238}U$ age of 56.19 ± 0.09 Ma.

4.7. 16FD708 (543011mE, 6594197mN; drill hole BCGE 08-05)

A suite of monzodiorite dikes in the Engineer mine area are cut by gold-bearing veins (ca. 49 Ma; Millonig et al., 2017). These dikes are also crosscut by a structure that transects the mine area. We collected a core sample of monzodiorite from drilling conducted by BCGold Corp. that was stored on site (drill hole 08-05, elevation 769m, azimuth 042°, dip 58º, and sample depth from 63 to 63.75m). The sample is from the most strongly altered variant of the suite, a white fine-grained feldspar-phyric dike with pervasive silica-white mica alteration, disseminated pyrite and green illite-lined fractures. Fine mafic phenocryst domains are replaced by carbonate-chlorite-quartz-opaques. These dikes are historically referred to as ‘rhyolite’.

The sample yielded prismatic igneous zircons and five single grains overlap on concordia with a weighted mean age of 54.48 ± 0.06 Ma (MSWD=0.53; n=5).

5. Geochemistry

The Coast Plutonic Complex is locally crosscut by gabbro to diorite dikes (Ootes et al., 2017), and K-Ar whole rock and biotite dating indicate some of these were emplaced at ca. 51 Ma (Symons et al., 2000). These dikes may be related to early Eocene volcanism and gold mineralization along the Llewellyn fault (Ootes et al., 2017). The dikes are all sub-vertical but have three distinct strikes (Fig. 2), north (010°, n=3), northeast (040° to 055°, n=6), and east-southeast (110°, n=3). In 2016, several dikes were sampled for whole rock geochemistry. In 2017 and 2018 we collected Sloko Group volcanic rock samples (Eocene; ca. 54 Ma; section 4.7; Mihalynuk et al.,1999) which outcrop at Engineer Mountain and south of Atlin Lake, for geochemical analysis.

Radiogenic isotope data were collected from a subset of samples that were analyzed for whole rock major and trace element geochemistry. Geochemical results are in Appendix 2.

5.1. Whole-rock major and trace element methods

Samples were prepared as chips in the field, then crushed and pulverized at the British Columbia Geological Survey. About 100 grams of each crushed and split sample was submitted to Activation Laboratories (Actlabs; Ancaster, Ontario) for whole rock major, trace, and rare earth element analysis. At Actlabs, the samples were further crushed to pass a 2 mm screen, mechanically split using a riffle splitter, and pulverized using a mild steel pulverizer to 95% passing 105 µm (code RX1). The resulting pulp was dissolved, and lithium metaborate/tetraborate fusion was performed to produce a molten bead, which was rapidly digested in a weak solution of nitric acid. Major elements were determined by inductively coupled plasma optical emission spectroscopy (ICP-OES), and trace element concentrations were measured using inductively coupled plasma mass spectroscopy (ICP-MS; Code 4Lithores). Measurement accuracy was determined using certified standards provided by Actlabs. In addition, blind in-house standards provided by the British Columbia Geological Survey were analyzed with the unknowns.

Details of the precision and accuracy of these samples are simplified here from Van Wagoner et al. (2021). To quantify accuracy the percent relative difference between the measured value of the reference standards and the certified value were calculated. Major element accuracy is generally within 5% error, and typically less than 2%. The trace element and rare-earth element (REE) accuracy is typically within 10% error with a few exceptions. To determine precision, the relative standard deviations (%RSD) were calculated using the duplicate reference material. Major element precision is within 7% RSD and trace element measurements within 11%. Where it exceeds 11%, the elements are in low concentrations.

5.2. Radiogenic isotope (Nd-Sr-Pb) methods

From the whole rock geochemical samples six were selected for radiogenic isotope analysis. Whole rock samples were sent to the Isotope Geochronology and Geochemistry Research Centre (IGGRC), Carleton University, Ottawa, Ontario. Samples were prepared in a clean lab and were measured for the Sr, Nd and Pb isotope ratios using two Thermo-Finnigan mass spectrometers (a Neptune MC-ICP-MS and a Triton TIMS). Sample powders between 50 and 150 milligrams were dissolved in a mixture of concentrated HF and HNO_3 on the hotplate at 130°C for 72 hours before were evaporated to dryness; the residues then were re-dissolved in 7M HNO_3 and 6M HCl. Pb, Sr and Nd were sequentially separated following the ion exchange column procedures described in Cousens (1996), except that Nd was separated using the pre-slurry-packed 2ml LN-resin columns (Eichrom Technologies LLC, USA). In addition, a Sr-Spec resin (Eichrom Technologies, LLC, USA) column procedure was used to remove Rb from the Sr fractions. Lead, Nd, and Sr isotope ratios were measured with both MC-ICP-MS and TIMS. Strontium and Nd isotopic ratios were normalized against $^{86}Sr/^{88}Sr$=0.1194 and $^{146}Nd/^{144}Nd$=0.7219, respectively. Lead sample solutions measured on MC-ICP-MS were doped with Tl (in a mass ratio of Tl/Pb =1:4) and Pb isotope ratios were normalized against $^{203}Tl/^{205}Tl$=0.418922. $^{143}Nd/^{144}Nd$ ratios measured by the Neptune MC-ICP-MS were further normalized for offsets using bracketing JNdi-1 average values against an IGGRC's Triton's JNdi-1 average value of 0.512100. Lead isotope ratios were also normalized for offsets using the bracketing NBS981 average values against the reference values of Todt et al., (1996).

For a period of 18 moths bracketing this analysis session, measurements of NBS987 and USGS standard BCR-2 yield average $^{87}Sr/^{86}Sr$ ratios, 0.710238±0.000024 (2SD, n=86) and 0.705009±0.000053 (2SD, n=7) with Neptune MC-ICP-MS; and 0.710242±0.000020 (2SD, n=45) and 0.704998±0.000018 (2SD, n=6) with Triton TIMS; measurements of JNdi-1(Tanaka et al., 2000) and BCR-2 give $^{143}Nd/^{144}Nd$ ratios, 0.512084±0.000010 (2SD, n=138) and 0.512626±0.000006 (2SD, n=4) with Neptune and 0.512100±0.000008 (2SD, n=49) 0.512623±0.000011 (n=7, 2SD) with Triton. NBS981 bracketing samples, yields average ratios of $^{206}Pb/^{204}Pb$=16.9321±0.0008 (2SD, n=17), $^{207}Pb/^{204}Pb$=15.4864±0.0008 (2SD, n=17), and $^{208}Pb/^{204}Pb$=36.6820±0.0023 (2SD, n=17). An analysis of BHVO-2 yields $^{206}Pb/^{204}Pb$=18.6286, $^{207}Pb/^{204}Pb$=15.5196, and $^{208}Pb/^{204}Pb$=38.1966. The total procedure blanks in IGGRC lab are <100pg, <250pg and <50 pg for Pb, Sr and Nd, respectively.

5.2.1. IGGRC Pb, Sr, Nd column procedure

Lead was separated and purified using AG1-X8 anionic resin using 1M HBr and 6M HCl. HBr wash solution was dried, and the residue was dissolved in 2.5 M HCl and loaded onto 14-ml Bio-Rad borosilicate glass chromatography columns containing 3.0 ml of AG50W-X8 cation resin. Columns were washed with 16 ml of 2.5 M HCl before Sr fractions were collected in 7 ml 2.5 M HCl; the columns were washed in 3.5 ml of 6M HCl before REE were eluted using 9 ml of 6M HCl. REE fractions were dissolved in 0.26M HCl and loaded onto Eichrom Ln Resin 2ml prepacked (slurry packed) chromatographic columns containing Teflon powder coated with HDEHP [di(2-ethylhexyl) orthophosphoric acid (Richard et al., 1976). Nd was eluted using 0.26M HCl. Sr fractions were cleaned to remove Rb using the Sr spec resin before measured on the Neptune MC-ICP-MS.

Acknowledgements

We thank Jessica Elliot and Reid Simmonds for assistance in the field and laboratory. We also thank R. Friedman for U-Pb zircon sample preparation and analysis at UBC-PCIGR assisted by H. Lin who did the U-Pb zircon mineral separation, and T. Ockerman who conducted activities in the clean lab and assisted with mass spectrometry.

References cited

Castonguay, S., Ootes, L., Devine, F., and Friedman, R., 2020. Superimposed Late Cretaceous and earliest Eocene gold mineralization and deformation events along the Llewellyn-Tally Ho deformation corridor in northwest British Columbia and southern Yukon. In: Mercier-Langevin, P., Lawley, C.J.M., and Castonguay, S., (Eds.), Targeted Geoscience Initiative 5: Contributions to the Understanding of Canadian Gold Systems. Geological Survey of Canada Open File 8712, pp. 223–236. https://doi.org/10.4095/326039

Colpron, M., 2020. Yukon Terranes - A digital atlas of terranes for the northern Cordillera. Yukon Geological Survey. https://data.geology.gov.yk.ca/Compilation/2#InfoTab

Cousens, B.L., 1996. Magmatic evolution of Quaternary mafic magmas at Long Valley Caldera and the Devils Postpile, California: Effects of crustal contamination on lithospheric mantle-derived magmas. Journal of Geophysical Research, 101, 27673-37689. https://doi.org/10.1029/96JB02093

Crowley, J.L., Schoene, B. and Bowring, S.A., 2007. U-Pb dating of zircon in the Bishop Tuff at the millennial scale. Geology, 35, 1123-1126.

Gerstenberger, H., and Haase, G., 1997. A highly effective emitter substance for mass spectrometric Pb isotopic ratio determinations. Chemical Geology, 136, 309-312.

Hart, C.J.R., and Radloff, J.K., 1990. Geology of Whitehorse, Alligator Lake, Fenwick Creek Carcross and part of Robinson map areas (105D/11, 6, 3, 2 & 7). Yukon Geological Survey, Open File 1990-4.

Jaffey, A.H., Flynn, K.F., Glendenin, L.E., Bentley, W.C., Essling, A.M., 1971. Precision measurement of half-lives and specific activities of ^{235}U and ^{238}U. Physical Review, C4, 1889-1906.

Mattinson, J.M., 2005. Zircon U-Pb chemical abrasion ("CA-TIMS") method: Combined annealing and multi-step partial dissolution analysis for improved precision and accuracy of zircon ages. Chemical Geology, 220, 47-66.

Mihalynuk, M.G., Mountjoy, K.J., Currie, L.D., Smith, M.T., and Rouse, J.N., 1999. Geology and mineral resources of the Tagish Lake area (NTS 104M/8, 9, 10E, 15 and 104N/12W) northwestern British Columbia. British Columbia Ministry of Employment and Investment, British Columbia Geological Survey Bulletin 105, 190p.

Millonig, L.J., Beinlich, A., Raudsepp, M., Devine, F., Archibald, D.A., Linnen, R.L., and Groat, L.A., 2017. The Engineer mine, British Columbia: An example of epithermal Au-Ag mineralization with mixed alkaline and subalkaline characteristics. Ore Geology Reviews, 83, 235-257.

Mundil, R., Ludwig, K.R., Metcalfe, I., and Renne, P.R., 2004. Age and timing of the Permian mass extinctions: U/Pb Dating of closed-system zircons. Science, 305, 1760-1763.

Ootes, L., Castonguay, S., Friedman, R., Devine, F., and Simmonds, R., 2018. Testing the relationship between the Llewellyn fault, Tally-Ho shear zone, and gold mineralization in northwest British Columbia. In: Geological Fieldwork 2017, British Columbia Ministry of Energy, Mines and Petroleum Resources, British Columbia Geological Survey Paper 2018-01, pp. 67-81.

Ootes, L., Elliott, J.M., and Rowins, S.M., 2017. Testing the relationship between the Llewellyn fault, gold mineralization, and Eocene volcanism in northwest British Columbia: A preliminary report. In: Geological Fieldwork 2016, British Columbia Ministry of Energy and Mines, British Columbia Geological Survey Paper 2017-1, pp. 49-59.

Richard, P., Shimizu, N., and Allègre, C.J., 1976. ^{143}Nd/^{146}Nd, a natural tracer: an application to oceanic basalts. Earth and Planetary Science Letters, 31, 269-278.

Scoates, J.S., and Friedman, R.M., 2008. Precise age of the platinuferous Merensky Reef, Bushveld Complex, South Africa, by the U-Pb ID-TIMS chemical abrasion ID-TIMS technique. Economic Geology, 103, 465-471.

Schmitz, M.D., and Schoene, B., 2007. Derivation of isotope ratios, errors, and error correlations for U-Pb geochronology using ^{205}Pb-^{235}U-(^{233}U)-spiked isotope dilution thermal ionization mass spectrometric data. Geochemistry, Geophysics. Geosystems, 8, article Q08006. https://doi.org/10.1029/2006GC001492

Stacey, J.S., and Kramers, J.D., 1975. Approximation of terrestrial lead isotopic evolution by a two-stage model. Earth and Planetary Science Letters, 26, 207–221.

Symons, D.T.A., Harris, M.J., Gabites, J.E., and Hart, C.J.R., 2000. Eocene (51 Ma) end to northward translation of the Coast Plutonic Complex: Paleomagnetism and K–Ar dating of the White Pass Dikes. Tectonophysics, 326, 93-109.

Tanaki, T., and 18 others, 2000. JNdi-1: A neodymium isotopic reference in consistency with LaJolla Neodymium. Chemical Geology, 168, 279-281. https://doi.org/10.1016/S0009-2541(00)00198-4

Thirlwall, M.F., 2000. Inter-laboratory and other errors in Pb isotope analyses investigated using a ^{207}Pb-^{204}Pb double spike. Chemical Geology, 163, 299-322.

Tizzard, A.M., Johnston, S.T., and Heaman, L.M., 2009. Arc imbrication during thick-skinned collision within the northern Cordilleran accretionary orogen, Yukon, Canada. In: Cawood, P. A., and Kröner, A. (Eds.), Earth Accretionary Systems in Space and Time. The Geological Society, London, Special Publications, 318, 309-327. https://doi.10.1144/SP318.11

Todt, W., R.A. Cliff, R.A., Hanser, A., and Hofmann, A.W., 1996, Evaluation of a ^{202}Pb–^{205}Pb double spike for high-precision lead isotope analysis, In Earth Processes: Reading the Isotopic Code Geophysical Monograph 95, the American Geophysical Union, pp. 159-174.

Van Wagoner, N., Ootes, L., and Sutcliffe, B., 2021. Geochemical data from the Kamloops Group. British Columbia Ministry of Energy, Mines and Low Carbon Innovation, British Columbia Geological Survey GeoFile 2021-16, 2p.

BRITISH COLUMBIA
Ministry of
Mining and
Critical Minerals

BRITISH COLUMBIA
est. 1895
GEOLOGICAL SURVEY